Biogeosciences Discuss., 8, 6519–6554, 2011
www.biogeosciences-discuss.net/8/6519/2011/
doi:10.5194/bgd-8-6519-2011

Biogeosciences
Discussions

Soil moisture control over autumn season methane flux, Arctic Coastal Plain of Alaska

C. S. Sturtevant[1], **W. C. Oechel**[1], **D. Zona**[2], **and C. E. Emerson**[3]

[1]Global Change Research Group, Department of Biology, San Diego State University, San Diego, California, USA
[2]Research Group of Plant and Vegetation Ecology, University of Antwerp, Wilrijk, Belgium
[3]San Diego State University, San Diego, California, USA

Received: 31 May 2011 – Accepted: 21 June 2011 – Published: 8 July 2011

Correspondence to: C. S. Sturtevant (sturteva@sciences.sdsu.edu)

Published by Copernicus Publications on behalf of the European Geosciences Union.

Abstract

Two shortfalls in estimating current and future seasonal budgets of methane efflux in Arctic regions are the paucity of non-summer measurements and an incomplete understanding of the sensitivity of methane emissions to changes in tundra moisture. A recent study in one Arctic region highlighted the former by observing a previously unknown large methane pulse during the onset of autumn soil freeze. This study addresses these research gaps by presenting an analysis of eddy covariance measurements of methane efflux and supporting environmental variables during the autumn season of 2009 and associated soil freeze-in period at our large-scale water manipulation site near Barrow, Alaska (the Biocomplexity Experiment). We found that methane emissions during the autumn were closely tied to liquid soil moisture in the top 30 cm of soil. Declines in soil moisture between manipulated wet, intermediate, and dry conditions as well as through time during the soil freeze-in period led to corresponding declines in methane efflux. During the period of soil freeze-in (from 23 September to 28 October), we estimate that our wet section emitted 623 mg CH_4 m^{-2} while the dry section emitted only 253 mg CH_4 m^{-2}, the average of which represents 18 % of net emissions from the typically measured growing season. We did not find evidence for a pulse in methane emissions during soil freeze at this site. Results from this study imply that future changes in tundra moisture will have a large effect on methane emissions in this region, and changes which span the saturation point are likely to have the largest effect. We speculate that changes in autumn soil moisture are also likely to affect winter emissions via the insulative effects of ice on winter soil temperature and liquid soil moisture availability after bulk soil freeze. Further research should expand the use of eddy covariance methane flux measurements to investigate ecosystem-level effects of tundra moisture on autumn and winter methane emissions in this and other Arctic regions.

1 Introduction

Methane (CH_4) is a potent greenhouse gas, exhibiting 25 times the 100-year global warming potential of CO_2 (Rodhe, 1990; Forster et al., 2007). Produced via decomposition under anaerobic conditions in moisture-saturated soils, methane emitted from wetlands is the largest single source of atmospheric methane world-wide (Denman et al., 2007). Northern wetlands contribute substantially to global wetland emissions. Of the estimated 100–231 Tg CH_4 yr^{-1} emitted from wetlands globally (Denman et al., 2007), Arctic and sub-Arctic tundra are thought to contribute 42 ± 26 Tg CH_4 yr^{-1} (Whalen and Reeburgh, 1992). This contribution from Arctic wetlands to atmospheric CH_4 may change significantly in the future as Arctic ecosystems are being rapidly and disproportionately altered by global warming (Abelson, 1989; Serreze et al., 2000; Trenberth et al., 2007). The fact that Arctic soils contain some of the largest soil organic carbon stocks which are already showing signs of increased availability for decomposition and release (Oechel et al., 1993; Schuur et al., 2009) further highlights the need to understand potential changes in CH_4 emissions from this region.

Moisture, temperature, and labile carbon supply are known to be the major factors influencing methane production in wetlands (Christensen et al., 2003), but the sensitivity of methane emissions to these factors remains uncertain (Walter and Heimann, 2000). Wetland methane emissions are predicted to be highly sensitive to climate change (Walter and Heimann, 2000), and this may be especially true for Arctic regions of near-surface permafrost (Roulet et al., 1992). In addition to changes in temperature and precipitation, the hydrological regime of Arctic ecosystems is likely to be substantially impacted due to permafrost thaw. Increases in the depth of seasonally thawed soil and evapotranspiration may lead to better drainage and a general lowering of the water table. On the other hand, ground subsidence instigated by the thawing of ice-rich permafrost (thermokarst) may result in more areas of poor drainage and high water retention (Schuur et al., 2008). The hydrological trajectory of continuous permafrost regions remains unclear, as changes have been observed in either direction (Smith et al., 2005; Jorgenson et al., 2006; Jones et al., 2009; Plug et al., 2008). Thus, forecasting future methane emissions from this region is beset by two key uncertainties: the direction of moisture change and the sensitivity of emissions to this change.

Particularly understudied periods of time concerning methane emissions from Arctic tundra are the shoulder (spring and autumn) and winter seasons, due in large part to the difficulty in maintaining measurements during these times. Most previous investigations have simply considered the ~100-day growing season, basing yearly estimates entirely from this time period (e.g. Sebacher et al., 1986) or extrapolating reduced fluxes throughout the off-season (e.g. Christensen, 1993). However, a recent study in Greenland observed an unexpected and extremely large methane pulse during autumn soil freeze (Mastepanov et al., 2008), suggesting that the currently held understanding of seasonal methane emission distribution in Arctic wetlands may need to be redefined.

The shoulder seasons represent transitions between high summer emissions and minimal winter emissions. These periods are important to investigate, not only because their study is needed to improve our understanding of seasonal and yearly methane emission estimates, but also because the rapidly changing environmental conditions during these times offer an opportunity to investigate the sensitivity of in-situ methane emissions to certain environmental factors. Understanding the factors which influence the rate and timing of emission transitions will improve the prediction of future growing season emissions as well as how the transitions themselves may change to affect net yearly emissions.

We had an opportunity to investigate methane efflux during one of the shoulder seasons under different tundra moisture conditions at our large-scale water table manipulation site near Barrow, Alaska (the Biocomplexity Experiment) during the autumn season of 2009. The Biocomplexity Experiment was initiated to examine the whole-ecosystem effects of altered tundra moistures on carbon storage and release by directly manipulating the water table at the ecosystem level. This site is of particular relevance to methane flux because most studies of methane flux in Arctic tundra have been conducted at the chamber- or sub-meter scale, identifying components of

Title Page
Abstract Introduction
Conclusions References
Tables Figures
◀| |▶
◀ ▶
Back Close
Full Screen / Esc
Printer-friendly Version
Interactive Discussion

tundra emissions and controls at the microtopographic level (e.g. Morrissey and Livingston, 1992; Whalen and Reeburgh, 1992; Christensen, 1993; Christensen et al., 2003; Kutzbach et al., 2004; Mastepanov et al., 2008; von Fischer et al., 2010). While these studies are incredibly important to advances in our understanding of controls and spatial variability, few have been able to measure Arctic methane emissions at the landscape scale (Wille et al., 2008; Fan et al., 1992; Friborg et al., 2000), not to mention experimentally attributing differences in methane flux to hydrologic change (Strack and Waddington, 2007). The Biocomplexity Experiment is therefore useful for improving our understanding of how small-scale processes and spatial heterogeneity in methane flux integrate to form the cumulative ecosystem response to general shifts in tundra moisture.

Normally our active measurements at this site conclude in August with the end of the growing season, but in light of the recently observed autumn methane pulse in the Greenland Arctic (Mastepanov et al., 2008) and an opportunity to use pre-production versions of a newly developed and now commercially available open-path methane analyzer, we conducted autumn eddy covariance measurements. For a study of growing season methane efflux conducted at this site, the reader is referred to Zona et al. (2009). In this study, our measurements investigate ecosystem-level fluxes of methane during the period of soil freeze-in when most biological activity in this Arctic landscape is generally thought to be shutting down for the winter. This paper discusses our flux observations in relation to environmental controls, showing how different tundra moisture regimes affect CH_4 emissions in this transition period due to combined changes in biotic and abiotic factors. Using our observations, we discuss the implications for autumn and winter methane emissions on the Arctic Coastal Plain of Alaska.

2 Site Description

2.1 General region

The Biocomplexity Experiment is located at the northern tip of Alaska near the village of Barrow. The terrain in this region mostly consists of poorly drained, polygonized acidic wet meadow tundra of minimal relief dominated by grasses, sedges, and mosses along with a few prostrate dwarf shrubs (Muller et al., 1999; Raynolds et al., 2005). The Gelisol soils are reworked, unconsolidated Quaternary marine sediments (Black, 1964) with major taxons of Typic Aquiturbel, Typic Histoturbel, and Typic Aquorthel (Bockheim et al., 1999). Annual average temperature and precipitation (1971 to 2000) are −12 °C and 106 mm, respectively; monthly maximums occur in July at 5 °C and August at 26 mm. The area is underlain by continuous permafrost and active layer depth (seasonally thawed ground) ranges from 30 to 90 cm (Bockheim et al., 1999). Snow melt typically occurs in the first week of June and freeze-up occurs in late September and October.

2.2 Biocomplexity Experiment site

Methane fluxes were recorded at the Biocomplexity Experiment site ("BE", Fig. 1). This experiment was initiated in 2005 and is the largest water table manipulation experiment ever conducted in the Arctic. This site is located within the Barrow Environmental Observatory about 6 km east of Barrow village and 6.5 km south of the Arctic Ocean (71°17′2.6″ N, 156°35′45.6″ W). The BE is centered on a vegetated thaw lake basin estimated to have drained 50 to 300 years before present (Hinkel et al., 2003).

Thaw lake basins form when one of the numerous and typically shallow lakes in this region drain as a result of several potential mechanisms, including stream capture or erosion of an outlet channel (Cabot, 1947; Carson, 1968). The lakes themselves are thought to originate due to local permafrost thaw and wind-driven expansion (Cabot, 1947; Carson, 1968). After drainage, the basin undergoes a several thousand year evolution of ice wedge polygon growth, changing soil characteristics, vegetation colonization and succession, and perhaps eventually lake re-formation (Billings and Peterson, 1980; Hinkel et al., 2003; Jorgenson and Shur, 2007). An aerial view of the Barrow Peninsula (and the Arctic Coastal Plain of Alaska in general) will reveal a collage-like landscape of lakes and vegetated drained basins that drained at various times in the past 5,500 years (Carson, 1968; Hinkel et al., 2003). Together, thaw lakes and vegetated thaw lake basins account for 66–72 % of the land surface in the Barrow region (Hussey and Michelson, 1966; Frohn et al., 2005), making this site generally representative of a large proportion of the Arctic Coastal Plain.

The BE basin (Fig. 1) is approximately 1.4 km long × 0.3 km wide, oriented in a north-south direction. The basin is of minimal relief, with the lower portions of the basin set less than 1.5 m below the surrounding tundra. Within the basin there is low to moderate ice wedge polygon development, and vegetation is dominated by *Sphagnum* mosses and wet and moist vascular communities (*Carex Aquatilis*, *Eriophorum scheuchzeri*, *Dupontia fisherii*, *Arctophila fulva*) (Olivas et al., 2010).

A large amount of infrastructure was installed at this site to investigate the ecological impacts of altered tundra moisture regimes (Fig. 1). In the spring of 2007 the BE basin was divided into three sections (North, Central, and South) by dikes. Two sets of dikes were inserted into the permafrost extending from the east to west edges of the basin to restrict the movement of water toward the natural drainage at the southern end (Zona et al., 2009) and to isolate the water tables in each section. Boardwalks run along the western edge of the basin as well as in three east-west transects to enable frequent sampling in each section without damage to the tundra. An eddy covariance tower is located in the west of each section, as prevailing winds are from the east.

3 Materials and methods

3.1 Water table manipulation

The objective of the manipulation was to increase the water table by 15 cm in the North section, decrease the water table by 15 cm in the Central section, and have the South section serve as a control or intermediate water table. Results will be presented in reference to these sections (North, Central, South). Treatment was conducted by pumping water from ponded low-center polygons in the Central section to the North section using high capacity pumps and hoses, beginning immediately after snowmelt and until surface water could no longer be removed (due to water removal as well as the natural drop in water table as thaw depth increased). In 2008 and 2009 additional water was pumped from a nearby pond into the North section, and in July of 2009 water was also added to the South section, the purpose in both cases to maintain or create differences in water tables. Summarizing for the 2009 treatment: approximately 9700 m^3 of water was pumped from the Central section to the North section between 4 June and 24 June, an additional 6800 m^3 of water was pumped into the North section from the nearby pond between 24 June and 24 July, and 1800 m^3 was pumped into the South section from this pond between 28 July and 8 August.

Although treatment activities were maintained in all three years of the manipulation (2007, 2008, and 2009), interannual differences in water availability and climatic conditions caused the treatment effects to differ between years and from target values (Olivas et al., 2010). However, in 2008 and 2009 the desired direction of change for all sections was achieved, for the entirety of the 2008 growing season and after late July in 2009. For detailed information on the history of the water table manipulation prior to the 2009 growing season, please see Olivas et al. (2010).

3.2 Eddy covariance Instrumentation

Fluxes of CH_4, CO_2, and H_2O were measured at a height of 1.9 m above the terrain using traditional eddy covariance instrumentation with the addition of a newly developed open-path CH_4 analyzer. Flux data were taken at 10 Hz and recorded with a datalogger. Three-dimensional wind speed and virtual sonic temperature were collected with a CSAT3 sonic anemometer (Campbell Scientific, Logan, Utah, USA). Molar densities of CO_2 and H_2O were collected with an open-path LI-7500 infrared gas analyzer (LI-COR Biosciences, Lincoln, NE, USA). Methane molar density was measured with a pre-production version of the now-commercial open-path LI-7700 methane analyzer (LI-COR Biosciences, Lincoln, NE, USA). Our group has worked extensively with LI-COR since 2006 in testing prototype units of this instrument at this and nearby study sites. The pre-production units used in this study were nearly identical to the final production instruments and have shown performance characteristics well-suited to eddy covariance measurements (McDermitt et al., 2010).

Two methane analyzers were installed at the BE on 19 August 2009 in the North and South sections, respectively. We had expected the use of three of the methane analyzers for the autumn, one for each section, but technical problems constrained us to the use of two at a given time. Therefore, the North tower was outfitted with an analyzer from 19 August to 25 October while the time periods of the other two towers were limited by the availability of an instrument: from 19 August to 7 September for the South tower and from 9 September to 25 October for the Central tower. For clarity in presentation, most environmental data from each section will only be reported for the concurrent methane flux measurement periods.

The LI-7500 and LI-7700 gas analyzers were calibrated before and after the study period via a 2-point linear equation. Ultra high purity nitrogen was used as the zero for CH_4, CO_2, and H_2O. High precision gases with certification accuracy $< 1\,\%$ were used as span values for CH_4 (4 ppm in a balance of VOC-free air) and CO_2 (750 ppm in a balance of nitrogen). The span value for H_2O was generated with a LI-610 dew point generator (LI-COR Biosciences, Lincoln, NE, USA) using a dew point 5 °C below ambient air temperature.

3.3 Eddy covariance flux computations

Half-hourly flux calculations of methane, carbon dioxide, water vapour, energy, and momentum were made using the eddy covariance method (Baldocchi et al., 1988) and coded in MATLAB v. 7.2 (Mathworks, Natick, Massachusetts, USA). Prior to covariance computations for each half hour, the sonic anemometer coordinate frame was double-rotated to align with the mean streamline and signals from separate sensors were time-aligned by maximizing the cross-correlation between vertical wind speed and scalar concentration. Appropriate corrections were applied for the simultaneous vertical transfer of heat and water vapour (Webb et al., 1980; McDermitt et al., 2010) as well as for high frequency spectral loss due to sensor separation and path length averaging (Moore, 1986). A footprint model (Hsieh et al., 2000) was used to determine the typical upwind distance contributing to the flux, and identified that under typical conditions 80 % of measured fluxes could be attributed to the first 135 m of tundra upwind from the tower. No gap-filling was performed.

Quality control was applied pre- and post- flux computation. Raw data were despiked (> 6 standard deviations from the running mean) and removed of periods clearly demonstrating error due to heavy mist, rain, or snow. Computed fluxes were filtered according to stationarity and integral turbulence characteristics tests following Foken at al. (2004). Fluxes calculated under low turbulence conditions (friction velocity < $0.1\ \mathrm{m\,s^{-1}}$) or when winds flowed from outside the manipulation footprint were excluded.

Finally, the overall integrity of the fluxes passing automatic quality control was assessed by the flux cospectra and energy budget closure. Evaluation of the flux cospectra showed good agreement with the empirical curves of Kaimal et al. (1972). Energy budget closure included terms for sensible and latent heat fluxes, net radiation, and soil heat flux, and averaged 84 % prior to the onset of soil freeze, which is better than the average closure reported for eddy covariance studies (79 %; Wilson et al., 2002).

After the onset of freeze, energy closure averaged 159 %; however, this is consistent with additional energy release during the phase change from liquid water to ice within the soil column (Tanaka et al., 2003; Guo et al., 2011) in relation to low net radiation values.

After quality checks and exclusion of fluxes originating outside the manipulation area, a total of 1481 half-hourly flux measurements (all three sections combined) were retained for analysis. This represented 25 % of recorded data, which is not surprising given the adverse weather conditions and shifting winds experienced at this site during the study period. No substantial difference existed between the proportions of retained daytime and night-time measurements, nor did the number of retained measurements differ greatly between sections during the concurrent measurement periods.

3.4 Supporting environmental measurements

Flux measurements were accompanied by a suite of lower-frequency environmental measurements, which are recorded year-round in the vicinity of each tower and within the manipulation footprint. Air temperature and relative humidity were measured at 1.6 m height with a HMP45C probe with radiation shield (Vaisala, Helsinki, Finland). Atmospheric pressure was measured at the Central tower with a PTB 101B electronic barometer (Vaisala, Helsinki, Finland). Temperatures at the soil surface and 5 cm, 10 cm, 20 cm, and 30 cm depths were measured with type T thermocouples. Soil moistures were recorded at three depths (0–30 cm, 0–10 cm, and 20–30 cm) with CS616 time domain reflectometry probes (Cambell Scientific, Logan, Utah, USA). A 1.5 m tripod housed radiation instruments measuring: upwelling and downwelling global shortwave radiation (310–2800 nm) with CMP3 pyranometers (Kipp and Zonen, Delft, The Netherlands), upwelling and downwelling photosynthetically-active radiation (PAR, 400–700 nm) with LI-190 quantum sensors (LI-COR Biosciences, Lincoln, NE, USA), and net radiation (0.25–60 µm) with a Q7 net radiometer (REBS, Bellvue, Washington, USA). Ground heat flux at 2 cm depth was averaged over five HFT3 ground heat flux plates (REBS, Bellvue, Washington, USA). Finally, a TR-525M tipping rain gauge bucket measured liquid precipitation (Texas Electronics, Dallas, Texas, USA). These environmental variables were measured at 1 Hz and averaged into half-hour blocks.

During the growing season (prior to the autumn measurement period), water table position and thaw depth were recorded each week every 4 m along the entire length of the east-west boardwalks traversing each section. Water table position was measured relative to the base of the vegetation layer using 2.5 cm perforated PVC tubes installed in the permafrost. Depth of thaw was measured by inserting a pointed, graduated metal rod into the ground until reaching frozen soil. Water table and thaw depth measurements were not continued past 19 August (the start of the autumn measurement period) as support personnel were reduced to a minimum at the end of the growing season and accurate measurements would have become difficult after the surface had begun freezing.

3.5 Statistical analysis

Data were statistically analyzed in Systat v. 12 (Systat Software, Chicago, IL, USA). We used forward-stepwise general linear modelling to identify the major environmental predictors of variation in methane fluxes both among manipulation sections and throughout the autumn. Here, we combined all data (North, Central, and South sections for the entire measurement period) and natural log-transformed the methane fluxes with an added constant to satisfy homoscedacity and lack of trend in the residuals. Thirteen points of negative half-hourly methane flux values which served as outliers in the model were excluded from the analysis. An alpha level of 0.05 was used to add or remove variables in the stepwise model.

4 Results

4.1 Water table manipulation prior to the autumn measurement period

For the early- to mid-2009 growing season, high water tables were maintained in the North section but the early-season removal of water from the Central section did not create a significant difference in water table between the Central and South sections. However, water table offsets among all three sections were achieved after 29 July (Fig. 2) when additional water was pumped into the South section. On 19 August, the beginning of the study period reported herein, the average water table in the North (wet) section was 9.9 cm above the surface, which was about 7.5 cm higher than the South (intermediate) section and 16 cm higher than the Central (dry) section.

Thaw depths among the sections showed offsets throughout the 2009 growing season in response to the treatment: the deepest in the North section, followed by the South section, and finally the Central section with the shallowest (Fig. 2). At the beginning of the autumn study period on 19 August, average thaw depth in the North section was about 34 cm below the surface, which was about 5 cm deeper than the South section and 8 cm deeper than the Central section.

4.2 Environmental conditions during the autumn

Air temperature generally fell throughout the study period, dropping consistently below 0 °C after 19 September and reaching a minimum daily average for the study period of −8 °C on 21 October. Soil temperatures dropped rapidly toward 0 °C beginning 19 September, and the active layer began freezing around 23 September (Fig. 3d). Liquid soil moistures in the top 30 cm of soil steadily declined after soil freeze began, reflecting the phase change from liquid water to ice (Fig. 3b). Soil temperatures at 10 cm depth for both the North and Central sections dropped consistently below 0 °C beginning 19 October and soil temperatures at 20 and 30 cm depths began dropping steeply below 0 °C on 28 October (Fig. 3d). Soil temperature at 30 cm depth in the Central section remained frozen throughout the study period.

During the concurrent period of North and South section methane flux measurements (19 August to 7 September), soil moistures in the top 30 cm of soil were nearly identical at close to 100 % volumetric water content ("VWC"; Fig. 3b). This observation was consistent with mean water tables in both sections being above the surface at the beginning of the study period. Coinciding with the higher water table in the North section, soil temperature at 20 cm depth in this section averaged 0.75 °C above the South section for this period (Fig. 3d).

During the concurrent period of North and Central section methane flux measurements and prior to soil freeze (9 September to 23 September), North section soil moisture in the top 30 cm was about twice that of the Central section (Fig. 3b). Soil temperature at 20 cm depth showed a corresponding offset, with the North section averaging 1.1 °C higher than the Central (Fig. 3d). After the onset of soil freeze, both North and Central section soil moistures fell as liquid water was converted to ice, maintaining a near-consistent offset.

After the end of the autumn measurement period and into the winter, soil temperatures in each section dropped below zero at different rates; the Central section dropped more steeply at first than the North and was consistently > 1 °C lower throughout the winter at 20 cm depth (minimum winter soil temperature approx. -15 °C; data not shown). Consistent with previous work in Arctic tundra (Olsson et al., 2003), measurable liquid soil moisture in the top 30 cm persisted for a time into the winter season although all measured soil temperatures in this layer dropped steeply below 0 °C beginning 28 October. Liquid soil moisture in the North section dropped below 1 % VWC on 18 November, which was 5 days later than the Central section.

Wind speeds varied greatly during the autumn, ranging from calm conditions to 14 m s^{-1} (Fig. 3c). Winds were predominantly from the east but ranged from all sectors. Peak incoming shortwave radiation declined throughout the autumn (Fig. 3e), and average daily net radiation fell below 0 W m^{-2} beginning 27 September. A total of 48 mm of liquid precipitation fell at the BE during the autumn, mostly during late August and early September. Long term snow accumulation at Wiley Post-Will Rogers Memorial

Airport (approximately 6.5 km west of the BE) began on 16 October and reached 15 cm by 25 October.

4.3 Autumn methane flux

Methane fluxes generally declined throughout the autumn period (Fig. 3a). In the late summer/early autumn (until 7 September), methane emissions were fairly steady and similar between the North (wet) and South (intermediate) sections. The North section methane flux averaged 1.4 mg CH_4 m^{-2} hr^{-1} during this time, only 0.14 mg CH_4 m^{-2} hr^{-1} greater than the South section on average. These flux values during the early autumn were comparable to past growing season values measured with different instrumentation at this site (Zona et al., 2009) as well as in the general region (von Fischer et al., 2010) and for similar tundra on the Arctic Coastal Plain of Alaska (Vourlitis et al., 1994).

Methane fluxes in the North section generally continued at early autumn levels until the onset of soil freeze, at which point emissions notably declined, following the fall in liquid soil moisture until the end of the measurement period (Fig. 3a and b). Central (dry) section methane fluxes, although significantly lower than the North section, exhibited the same trend, averaging 0.58 mg CH_4 m^{-2} hr^{-1} prior to soil freeze and declining thereafter. Both the North and Central sections, however, continued to emit small levels of methane at the end of the study period, even though the soil was frozen past 10 cm depth by this time (Fig. 3a and d). During the entire period of concurrent North-Central methane flux measurements (9 September–25 October), the North section emitted methane at approximately 2.2 times the rate of the Central section, which corresponded well with the difference in soil moistures between these two sections.

Short periods of increased methane emission were observed throughout the autumn for all three sections, up to 4 mg CH_4 m^{-2} hr^{-1} in the North section, and coincided with periods of high wind speed. However, peak emissions were short-lived and very small compared to the strikingly large emissions that have been observed in the Greenland Arctic during soil freeze (Mastepanov et al., 2008). It was also noted that no large emissions were observed when winds shifted such that fluxes were representative of the surrounding tundra (data not shown), and these fluxes were generally lower than those measured from the BE basin. The area surrounding the BE basin is typical of the region, where the surrounding tundra is normally higher in elevation than the basin and better drained (Hussey and Michelson, 1966).

4.4 Relationship between environmental variables and autumn methane flux

From visual inspection of the data, the variation in methane fluxes among the manipulation sections and throughout the autumn showed a strong, positive correlation with soil moisture in the top 30 cm (Fig. 3a and b). It was also immediately noted that the short term peaks in methane flux corresponded to peaks in wind speed (Fig. 3a and c). Forward stepwise general linear modelling (GLM) using the combined data set from all three manipulation sections indeed confirmed that soil moisture in the top 30 cm and wind speed were the most significant in explaining the variation in methane flux at the BE during the autumn (Table 1). In addition to soil moisture and wind speed, soil temperature at 20 cm depth and incoming shortwave radiation (310–2800 nm) were also identified as environmental variables statistically contributing to the explained variation in methane flux. All four variables were positively related to methane efflux and, taken together, explained 70 % of the variation in half-hourly fluxes (Table 1).

Soil moisture in the top 30 cm was by far the major environmental variable explaining the variation in methane fluxes at the BE, alone explaining 62 % of the variation in half-hourly methane efflux (Table 1). High soil moisture in both the North (wet) and South (intermediate) sections coincided with similar methane flux, while the significantly lower soil moisture in the Central (dry) section corresponded to approximately half the methane emissions compared to the North section. In addition, the decline in liquid soil moisture during soil freeze in the North and Central sections was closely followed by a general decline in methane flux.

Wind speed was the second-most significant contributor to variation in methane flux at the BE, although to a much lesser degree than soil moisture alone. Wind speed had an interactive effect with soil moisture, this interaction term contributing 3.5 % to the explained variation after soil moisture was added to the GLM (Table 1). Temporary peaks in methane efflux for all sections occurred during high wind events, and this effect was enhanced with the higher soil moisture levels in the North section as well as in the both the North and Central sections prior to the decline in liquid soil moisture during soil freeze.

Soil temperature at 20 cm depth and incoming shortwave radiation were the final statistically significant environmental variables contributing to the variation in methane flux (Table 1). Soil temperature contributed an additional 2.6 % to the explained variation, although its explanatory power was largely confined to its variation before freeze began (when temperature was constant at 0 °C). Greater methane efflux corresponded with higher soil temperatures (20 cm depth) both prior to soil freeze and under wetter conditions. Incoming shortwave radiation, contributing a final 1.6 % to the variation explained by the model, appeared to correspond with the timing of the small diurnal pattern in methane flux, both diurnals showing a peak during midday which decreased in magnitude throughout the autumn.

CO_2 flux was not used in the main GLM due to a lower number of fluxes passing quality control and therefore a reduction in sample size. However, when the reduced sample size GLM was run to include CO_2 flux with the previously identified significant predictors, CO_2 flux was identified as significant but entered the model last and only contributed 0.2 % to the total variation explained. This is fairly consistent with previous results at this site which found no relationship between methane flux and net ecosystem exchange of CO_2 (Zona et al., 2009).

4.5 Summary of key results

The water table manipulation at the BE created the desired effect on tundra moisture in the three experimental sections during the autumn season of 2009. These alternate tundra moistures corresponded with variations in other environmental conditions and methane efflux. The North section was the wettest with an average water table well above the surface in the early autumn. The North section exhibited the deepest depth of thaw and the highest mid-layer soil temperature (20 cm depth). This section had the highest observed methane fluxes throughout the autumn. The South section was intermediate in wetness with an average water table just above the surface in the early autumn, a thaw depth between that of the North and Central sections, and a soil temperature (20 cm depth) also intermediate to those of North and Central. South section methane fluxes were only measured in the early autumn and were only slightly lower than those of the North section. The Central section was the driest of the three sections, having also the shallowest depth of thaw and the lowest soil temperature at 20 cm depth. Methane fluxes in this section were measured for the latter two-thirds of the autumn and were substantially lower than those of the North section.

Methane fluxes declined throughout the autumn, most notably with the decline in liquid soil moisture during soil freeze. Methane fluxes were also positively related to wind speed, soil temperature at 20 cm depth, and incoming global shortwave radiation. No large pulse in methane emissions was observed for any section during the autumn. Small amounts of methane were still being emitted from this site at the end of our study period, although the soil had frozen past 10 cm depth. Liquid soil moisture in the top 30 cm existed well into the beginning of winter and persisted longer in the wetter North section compared to the drier Central. North section winter soil temperatures (20 cm depth) were also typically $>1\,^{\circ}$C higher than the Central throughout the winter.

5 Discussion

5.1 Controls over autumn CH_4 flux

CH_4 flux at the BE during the autumn season was closely tied to soil moisture in the active layer (top 30 cm). This strong correspondence of methane flux to soil moisture is not surprising given moisture's well-documented control over aerobic vs. anaerobic respiration and microbial processes in general. Indeed, von Fischer et al. (2010) found that soil moisture was the strongest predictor of CH_4 emission rate across a range of microsites on the tundra near Barrow, including sites on the non-manipulated tundra immediately surrounding the BE. Prior to soil freeze, soil moisture in the top 30 cm of soil was probably an excellent indicator of general position of the water table (up to the surface) and therefore the general oxygen availability within the active layer. Below the water table, diffusion of oxygen is slow and anaerobic conditions predominate, promoting organic matter decomposition via anaerobic pathways which include methanogenesis (Morrissey and Livingston, 1992). In addition, a higher water table reduces the layer of oxic soil between the water table and the atmosphere, thereby limiting the substantial microbial methane oxidation known to occur in this zone (Whalen and Reeburgh, 1990). Our data support that the generally subsurface water table in the Central section promoted less anaerobic decomposition and greater methane oxidation than the North and South sections (which exhibited generally above-surface water tables).

Although the average water table in the North section was well above the South section in the early autumn, North and South methane efflux were very similar. This observance and knowledge of the site may point to the role of microtopography in moderating methane efflux in a generally inundated landscape. The North section has greater polygon development than the South (as can be seen in Fig. 1), which manifests as greater microtopographic variation in the North (Fig. 4). Therefore, although the average water table in the North was 7.5 cm higher than the South section at the beginning of the measurement period, the greater range in surface elevations caused the proportion of individual locations with a water table below the surface to be nearly the same as the South (23 % vs. 25 %, respectively). This suggests that greater microtopography may limit increases in methane emission at high water tables by providing more aerobic microsites for methane oxidation to occur. It also suggests that changes in water table which cross the surface have the largest effect on methane emissions.

After the onset of soil freeze, soil moisture in the top 30 cm appeared to be an indicator of unfrozen moisture available for microbial activity. This is supported by the decline in methane efflux during soil freeze and the continuance of both liquid soil moisture and methane production at the end of the study period although all measured soil temperatures were at or below freezing. The latter is consistent with the persistence of microbial activity and liquid soil moisture down to −39 °C in Arctic tundra soils (Panikov et al., 2006; Oechel et al., 1997). Since liquid soil moisture in both the North and Central sections did not drop to near-zero levels until mid-November, measurable amounts of methane emission may have occurred until this time.

Soil temperature is known to have strong influence on microbial activity and methane efflux in Alaskan Arctic tundra (Morrissey and Livingston, 1992) and has been noted specifically for this site during the growing season (Zona et al., 2009). However, the virtually constant soil temperature (20 cm depth) at 0 °C during the long period of soil freeze did not allow for much of a controlling influence of temperature on variation in methane production. This does not necessarily suggest that autumn methane fluxes at the BE respond minimally to variation in soil temperature, simply that the stronger variation in other environmental variables during this time becomes more important. Indeed, the identification of increased soil temperature as a significant, albeit small, contributor to increases in methane efflux despite the fact that temperatures were constant for a large proportion of the study period would seem to highlight its importance.

Increased soil temperature observed with increased wetness (Central < South < North) was a result of heat conduction to the deep soil by water. This has been established both experimentally at this site (Zona et al., 2009; Olivas et al., 2010) and observationally in other studies (Walker et al., 2003; von Fischer et al., 2010). Increased heat conduction to the soil not only increases the temperature of deeper soil layers but also deepens the active layer at a faster rate. Soils in this region maintain high organic carbon contents throughout the top 100 cm of soil (Bockheim et al., 1999), therefore a larger volume of unfrozen soil provides a greater amount of organic carbon available for decomposition (Vourlitis et al., 1993; Zona et al., 2009). Thus, although we could not add thaw depth as an explanatory variable in the GLM due to measurements ending on 19 August, the soil moisture-induced greater thaw depth under wetter conditions (Central < South < North) probably also contributed to corresponding increases in methane efflux. The higher mid-layer soil temperature (20 cm depth) and greater thaw depth in the North section may explain the slightly higher North section methane efflux compared to the South.

The effect of wind speed on CH_4 flux is assumed to be a physical mechanism promoting the release of microbially-respired methane from the soil column rather than a biological control of methane production. Higher wind speeds disturb emergent vegetation, which may instigate the release of methane bubbles trapped in the top layer of soil or within graminoid stems. Morrissey and Livingston (1992) observed that winds of approximately $10\,\mathrm{m\,s^{-1}}$ or greater instigated methane ebullition in Alaskan Arctic tundra. Our observations probably included varying degrees of this effect. The enhancement of the wind speed effect on CH_4 flux at higher soil moistures is likely due to the fact that a greater amount of respired methane was available for release in wetter conditions.

5.2 No observed autumn methane pulse

No autumn methane pulse was observed at the Biocomplexity Experiment site under high or low soil moisture conditions. Nor did we observe any evidence of a burst when shifting winds caused fluxes to be measured for short periods from the surrounding tundra. Instead of a drastic increase in methane emission as the active layer froze, we observed a general decline in emissions punctuated by small increases during high wind events.

Why did we not observe an autumn methane pulse? One explanation may simply be that a substantial amount of methane is not stored within the tundra in this region and any that is trapped throughout the growing season is released during disturbance from high wind events. Methane fluxes measured with the eddy covariance method represent fluxes integrated over a large area, and considering fetch and shifting wind directions, measured fluxes over the course of the autumn were representative of a large proportion of each manipulation section (tens of thousands of square meters). Therefore, another explanation is that high-concentration bubbles of methane were forced out of freezing soil at point locations at the BE but amounted to little noticeable release when averaged over the large flux footprint.

Finally, it is possible that large quantities of methane were not released by the system until after our measurement period had ended. However, we do not think this to be the case: The active layer at this site is shallow; soil freeze-up of the ca. 30 cm–40 cm active layer occurs simultaneously from both the top-down and bottom-up (Mackay, 1983; Hinzman et al., 1991). Soil moisture measurements indicated that almost 60 % of the available pore water in the entire Central section active layer had frozen by 21 October, the last date of acceptable methane flux measurements at the BE. In the North section over 40 % of the available pore water in the top 30 cm of soil, plus the entire ~10 cm of surface water, had frozen by this time. Therefore, much of the methane stored in the system should have been frozen out during our measurement period.

5.3 Implications

Our data are consistent with the body of evidence that active layer soil moisture is a predominant control on methane efflux in Arctic regions (e.g. Morrissey and Livingston, 1992; Christensen, 1993; Vourlitis et al., 1993; von Fischer et al., 2010). However, this study extends those observations into the autumn season soil freeze-up, and integrates over a larger landscape unit for a surface type which is generally representative of a large part of the Arctic Coastal Plain of Alaska. While this study is limited to a site with footprints in close proximity, the study benefits from its ability to integrate within-ecosystem heterogeneity, and therefore provides a comprehensive picture of the net-ecosystem response over approximately 0.4 km^2 to environmental conditions. The ecosystem-level effects we observed due to large changes in tundra moisture are likely to apply to a large proportion of similar landforms on the Arctic Coastal Plain and therefore have probable implications for this region's seasonal and yearly methane budget under current conditions as well as global change.

Using our regression results to obtain a cumulative estimate of methane emissions from the onset of soil freeze until soil temperatures began dropping steeply below

$0\,^{\circ}\mathrm{C}$ (23 September to 28 October), we arrive at $623\,\mathrm{mg\,CH_4\,m^{-2}}$ emitted for the North section and $253\,\mathrm{mg\,CH_4\,m^{-2}}$ for the Central section. The average of these, $438\,\mathrm{mg\,CH_4\,m^{-2}}$, represents a conservative estimate of methane efflux typically not measured as part of the growing season, and amounts to 18 % of the 100-day cumulative summer methane efflux we computed from previously measured emissions at this site (Zona et al., 2009). Therefore, while the autumn-winter transition exhibits dwindling methane emissions, it still represents a measureable component of the yearly budget and should be considered, along with winter rates, in studies of methane efflux from Arctic tundra.

In a future Arctic, our results suggest that should a general drying of the Arctic Coastal Plain cause water tables to drop from above to below the surface, CH_4 efflux will be substantially reduced. Wet sites with high graminoid cover, similar to this one, are the dominant CH_4 emitters in the region (Morrissey and Livingston, 1992). Reducing the 6.3–7.2 $\mathrm{Tg\,CH_4\,yr^{-1}}$ (Christensen, 1993) of wet meadow tundra emissions by half (as seen in this study under dry vs. wet conditions) would reduce net Arctic and sub-Arctic tundra emissions by ~8 %. We see this as a conservative reduction, since emissions from the much larger area of moist tundra would also likely be reduced under drier conditions. Conversely, a shift to wetter ecosystems from drier tundra will likely cause a substantial increase in emissions, especially where water tables increase from below to above the surface in areas of low microtopography. These predicted effects are from a shift in tundra moisture alone, and are sure to be accompanied by short- and long-term effects from ecosystem changes induced by warmer air temperatures, thermokarst erosion, rising CO_2 levels, shifts in vegetation, and many other factors.

The effect of autumn soil moisture on winter soil temperature may be of significant importance for winter methane emissions. Cold season respiration in Arctic soils can be significant when integrated over the entire season (Oechel et al., 1997). Respiration in soils near Barrow has been shown to exponentially increase with temperature from temperatures as low as $-39\,^{\circ}\mathrm{C}$ (Panikov et al., 2006). After temperatures in the soil column began to drop steeply below $0\,^{\circ}\mathrm{C}$ after the autumn study period, those in the drier Central section fell faster and deeper as well as remained more than 1 °C lower throughout the winter when compared with the wetter North section. This was due to the insulative effects of ice, where greater autumn soil moisture in the North resulted in a greater ice volume above and within the soil, which better insulated the soil from the harsh winter temperatures. This implies that winter methane emissions are also likely to be affected by altered tundra moistures, and may become significant when integrated over the entire cold season. Winter microbial activity may be significantly reduced under drier conditions due to colder soil temperatures, whereas winter microbial activity is likely to increase in wetter conditions that promote more favourable soil temperatures. Under a future scenario of warmer and wetter tundra, this effect and the additional persistence of liquid soil moisture well into the start of winter may increase autumn and winter emissions enough to substantially affect yearly estimates.

Finally, the lack of evidence for an autumn methane pulse under relatively wet or dry conditions implies that high autumn methane emissions during soil freeze may not be generally applicable to wet meadow tundra ecosystems with near-surface permafrost. The improvement of measured vs. modelled high latitude methane concentrations when an autumn pulse was included (as reported in Mastepanov et al., 2008) lends merit to its widespread application; however, further research should continue to investigate where and under what conditions this strong seasonal dynamic is apparent so that global methane transport models as well as mechanistic Arctic emission models may be improved.

6 Conclusions

This study investigated the role of soil moisture and other environmental factors in influencing ecosystem-level methane emissions in Arctic wet meadow tundra at a time when the ecosystem was generally shutting down for the winter. We measured methane fluxes at the Biocomplexity Experiment site during the autumn and associated soil freeze period with the use of a newly developed open-path methane analyzer (now commercially available as the LI-COR 7700). We found a general decline in emissions throughout the autumn and that liquid soil moisture in the active layer was by far the most significant predictor of methane efflux, able to explain general emission differences between manipulated wet, intermediate, and dry tundra as well as the decline in emissions during the soil freeze-in period. The main implications of these findings are that although we found no evidence for an autumn methane pulse, the autumn was found to be an important component of yearly methane emissions, and a change to tundra moisture availability in either direction as a result of global change is likely to substantially affect autumn methane emissions in this region. Changes in moisture which span the saturation point are likely to have the largest effect. In addition, we speculate that winter emissions are also likely to be influenced by changes in tundra moistures, owing to moisture's effect on soil temperature and liquid moisture availability into the winter season. Further research should expand the use of eddy covariance methane flux measurements to investigate the effect of tundra moisture on autumn and winter methane emissions at the ecosystem-level in this and other Arctic regions.

Acknowledgements. We would like to thank LI-COR Biosciences for the opportunity to use the newly developed LI-7700 methane analyzer as well as their technical assistance in doing so. We also thank the Barrow Arctic Science Consortium and CH2M Hill Polar Services for logistic support, as well as the many undergraduates and personnel who contributed to maintaining this experiment site. This research was made possible by support from the National Science Foundation Office of Polar Programs (Grant No. OPP-0436177), the US Department of Energy National Institute for Climate Change Research (Grant No. DE-FC02-06ER64159), and the National Science Foundation Graduate Research Fellowship (under Grant No. DGE-0738622).

References

Abelson, P. H.: The Arctic – a key to world climate, Science, 243, 873–873, 1989.

Baldocchi, D. D., Hicks, B. B., and Meyers, T. P.: Measuring biosphere-atmosphere exchanges of biologically related gases with micrometeorological methods, Ecology, 69, 1331–1340, 1988.

Billings, W. D. and Peterson, K. M.: Vegetational change and ice-wedge polygons through the thaw-lake cycle in Arctic Alaska, Arct. Alp. Res., 12, 413–432, 1980.

Black, R. F.: Gubik formation of Quaternary age in northern Alaska, US Geol. Surv. Prof. Paper, 302-C, 59–91, 1964.

Bockheim, J. G., Everett, L. R., Hinkel, K. M., Nelson, F. E., and Brown, J.: Soil organic carbon storage and distribution in Arctic Tundra, Barrow, Alaska, Soil Sci. Soc. Am. J., 63, 934–940, 1999.

Cabot, E. C.: The northern Alaskan coastal plain interpreted from aerial photographs, Geogr. Rev., 37, 639–648, 1947.

Carson, C. E.: Radiocarbon dating of lacustrine strands in Arctic Alaska, Arctic, 21, 12–26, 1968.

Christensen, T. R.: Methane emission from Arctic tundra, Biogeochemistry, 21, 117–139, 1993.

Christensen, T. R., Ekberg, A., Strom, L., Mastepanov, M., Panikov, N., Oquist, M., Svensson, B. H., Nykanen, H., Martikainen, P. J., and Oskarsson, H.: Factors controlling large scale variations in methane emissions from wetlands, Geophys. Res. Lett., 30, 1414, doi:10.1029/2002GL016848, 2003.

Denman, K. L., Brasseur, G., Chidthaisong, A., Ciais, P., Cox, P. M., Dickinson, R. E., Hauglustaine, D., Heinze, C., Holland, E., Jacob, D., Lohmann, U., Ramachandran, S., da Silva Dias, P. L., Wofsy, S. C., and Zhang, X.: Couplings Between Changes in the Climate System and Biogeochemistry, in: Climate Change 2007: The Physical Science Basis. Contribution of Working Group I to the Fourth Assessment Report of the Intergovernmental Panel on Climate Change, edited by: Solomon, S., Qin, D., Manning, M., Chen, Z., Marquis, M., Averyt, K. B., Tignor, M., and Miller, H. L., Cambridge University Press, Cambridge, United Kingdom and New York, NY, USA, 2007.

Fan, S. M., Wofsy, S. C., Bakwin, P. S., Jacob, D. J., Anderson, S. M., Kebabian, P. L., McManus, J. B., Kolb, C. E., and Fitzjarrald, D. R.: Micrometeorological measurements of CH_4 and CO_2 exchange between the atmosphere and sub-arctic tundra, J. Geophys. Res.-Atmos., 97, 16627–16643, 1992.

Foken, T., Gockede, M., Mauder, M., Mahrt, L., Amiro, B., and Munger, W.: Post-field data quality control, in: Handbook of micrometeorology: a guide for surface flux measurement and analysis, edited by: Lee, X., Massman, W. J., and Law, B. E., Kluwer Academic Publishers, Dordrecht, 2004.

Forster, P., Ramaswamy, V., Artaxo, P., Berntsen, T., Betts, R., Fahey, D. W., Haywood, J., Lean, J., Lowe, D. C., Myhre, G., Nganga, J., Prinn, R., Raga, G., M., S., and Van Dorland, R.: Changes in Atmospheric Constituents and in Radiative Forcing, in: Climate Change 2007: The Physical Science Basis. Contribution of Working Group I to the Fourth Assessment Report of the Intergovernmental Panel on Climate Change, edited by: Solomon, S., Manning, M., Chen, Z., Marquis, M., Averyt, K. B., Tignor, M., and Miller, H. L., Cambridge University Press, Cambridge, United Kingdom and New York, NY, USA, 2007.

Friborg, T., Christensen, T. R., Hansen, B. U., Nordstroem, C., and Soegaard, H.: Trace gas exchange in a high-arctic valley 2. Landscape CH_4 fluxes measured and modeled using eddy correlation data, Global Biogeochem. Cy., 14, 715–723, 2000.

Frohn, R. C., Hinkel, K. M., and Eisner, W. R.: Satellite remote sensing classification of thaw lakes and drained thaw lake basins on the North Slope of Alaska, Remote Sens. Environ., 97, 116–126, doi:10.1016/j.rse.2005.04.022, 2005.

Guo, D., Yang, M., and Wang, H.: Characteristics of land surface heat and water exchange under different soil freeze/thaw conditions over the central Tibetan Plateau, Hydrol. Process., 25, doi:10.1002/hyp.8025, 2011.

Hinkel, K. M., Eisner, W. R., Bockheim, J. G., Nelson, F. E., Peterson, K. M., and Dai, X. Y.: Spatial extent, age, and carbon stocks in drained thaw lake basins on the Barrow Peninsula, Alaska, Arct. Antarct. Alp. Res., 35, 291–300, 2003.

Hinzman, L. D., Kane, D. L., Gieck, R. E., and Everett, K. R.: Hydrologic and thermal-properties of the active layer in the Alaskan Arctic, Cold. Reg. Sci. Technol., 19, 95–110, 1991.

Hsieh, C. I., Katul, G., and Chi, T.: An approximate analytical model for footprint estimation of scaler fluxes in thermally stratified atmospheric flows, Adv. Water. Resour., 23, 765–772, 2000.

Hussey, K. M. and Michelson, R. W.: Tundra relief features near point Barrow Alaska, Arctic, 19, 162–184, 1966.

Jones, B. M., Arp, C. D., Hinkel, K. M., Beck, R. A., Schmutz, J. A., and Winston, B.: Arctic lake physical processes and regimes with implications for winter water availability and management in the National Petroleum Reserve Alaska, Environ. Manage., 43, 1071–1084, doi:10.1007/s00267-008-9241-0, 2009.

Jorgenson, M. T. and Shur, Y.: Evolution of lakes and basins in northern Alaska and discussion of the thaw lake cycle, J. Geophys. Res.-Earth., 112, F02s17, doi:10.1029/2006jf000531, 2007.

Jorgenson, M. T., Shur, Y. L., and Pullman, E. R.: Abrupt increase in permafrost degradation in Arctic Alaska, Geophys. Res. Lett., 33, L02503, doi:10.1029/2005gl024960, 2006.

Kaimal, J. C., Izumi, Y., Wyngaard, J. C., and Cote, R.: Spectral characteristics of surface-layer turbulence, Q. J. Roy. Meteor. Soc., 98, 563–589, 1972.

Kutzbach, L., Wagner, D., and Pfeiffer, E. M.: Effect of microrelief and vegetation on methane emission from wet polygonal tundra, Lena Delta, Northern Siberia, Biogeochemistry, 69, 341–362, 2004.

Mackay, J. R.: Downward water-movement into frozen ground, western Arctic coast, Canada, Can. J. Earth Sci., 20, 120–134, 1983.

Mastepanov, M., Sigsgaard, C., Dlugokencky, E. J., Houweling, S., Strom, L., Tamstorf, M. P., and Christensen, T. R.: Large tundra methane burst during onset of freezing, Nature, 456, 628–658, doi:10.1038/nature07464, 2008.

McDermitt, D., Burba, G., Xu, L., Anderson, T., Komissarov, A., Riensche, B., Schedlbauer, J., Starr, G., Zona, D., Oechel, W., Oberbauer, S., and Hastings, S.: A new low-power, open-path instrument for measuring methane flux by eddy covariance, Appl. Phys. B.-Lasers O., 1–15, doi:10.1007/s00340-010-4307-0, 2010.

Moore, C. J.: Frequency-response corrections for eddy-correlation systems, Bound.-Lay. Meteorol., 37, 17–35, 1986.

Morrissey, L. A. and Livingston, G. P.: Methane emissions from Alaska Arctic tundra – an assessment of local spatial variability, J. Geophys. Res.-Atmos., 97, 16661–16670, 1992.

Muller, S. V., Racoviteanu, A. E., and Walker, D. A.: Landsat MSS-derived land-cover map of northern Alaska: extrapolation methods and a comparison with photo-interpreted and AVHRR-derived maps, Int. J. Remote Sens., 20, 2921–2946, 1999.

Oechel, W. C., Hastings, S. J., Vourlitis, G., Jenkins, M., Riechers, G., and Grulke, N.: Recent change of Arctic tundra ecosystems from a net carbon-dioxide sink to a source, Nature, 361, 520–523, 1993.

Oechel, W. C., Vourlitis, G., and Hastings, S. J.: Cold season CO_2 emission from arctic soils, Global Biogeochem. Cy., 11, 163–172, 1997.

Olivas, P. C., Oberbauer, S. F., Tweedie, C. E., Oechel, W. C., and Kuchy, A.: Responses of CO_2 flux components of Alaskan Coastal Plain tundra to shifts in water table, J. Geophys. Res.-Biogeo., 115, G00i05, doi:10.1029/2009jg001254, 2010.

Olsson, P. Q., Sturm, M., Racine, C. H., Romanovsky, V., and Liston, G. E.: Five stages of the Alaskan Arctic cold season with ecosystem implications, Arct. Antarct. Alp. Res., 35, 74–81, 2003.

Panikov, N. S., Flanagan, P. W., Oechel, W. C., Mastepanov, M. A., and Christensen, T. R.: Microbial activity in soils frozen to below-39 degrees C, Soil. Biol. Biochem., 38, 785–794, doi:10.1016/j.soilbio.2005.07.004, 2006.

Plug, L. J., Walls, C., and Scott, B. M.: Tundra lake changes from 1978 to 2001 on the Tuktoyaktuk Peninsula, western Canadian Arctic, Geophys. Res. Lett., 35, L03502, doi:10.1029/2007gl032303, 2008.

Raynolds, M. K., Walker, D. A., and Maier, H. A.: Plant community-level mapping of arctic Alaska based on the Circumpolar Arctic Vegetation Map, Phytocoenologia, 35, 821–848, doi:10.1127/0340-269x/2005/0035-0821, 2005.

Rodhe, H.: A comparison of the contribution of various gases to the greenhouse-effect, Science, 248, 1217–1219, 1990.

Roulet, N., Moore, T., Bubier, J., and Lafleur, P.: Northern fens – methane flux and climatic-change, Tellus B., 44, 100–105, 1992.

Schuur, E. A. G., Bockheim, J., Canadell, J. G., Euskirchen, E., Field, C. B., Goryachkin, S. V., Hagemann, S., Kuhry, P., Lafleur, P. M., Lee, H., Mazhitova, G., Nelson, F. E., Rinke, A., Romanovsky, V. E., Shiklomanov, N., Tarnocai, C., Venevsky, S., Vogel, J. G., and Zimov, S. A.: Vulnerability of permafrost carbon to climate change: Implications for the global carbon cycle, Bioscience, 58, 701–714, doi:10.1641/b580807, 2008.

Schuur, E. A. G., Vogel, J. G., Crummer, K. G., Lee, H., Sickman, J. O., and Osterkamp, T. E.: The effect of permafrost thaw on old carbon release and net carbon exchange from tundra, Nature, 459, 556–559, doi:10.1038/nature08031, 2009.

Sebacher, D. I., Harriss, R. C., Bartlett, K. B., Sebacher, S. M., and Grice, S. S.: Atmospheric methane sources: Alaskan tundra bogs, an alpine fen, and a subarctic boreal marsh, Tellus B, 38B, 1–10, doi:10.1111/j.1600-0889.1986.tb00083.x, 1986.

Serreze, M. C., Walsh, J. E., Chapin, F. S., Osterkamp, T., Dyurgerov, M., Romanovsky, V., Oechel, W. C., Morison, J., Zhang, T., and Barry, R. G.: Observational evidence of recent change in the northern high-latitude environment, Clim. Change, 46, 159–207, 2000.

Smith, L. C., Sheng, Y., MacDonald, G. M., and Hinzman, L. D.: Disappearing Arctic lakes, Science, 308, 1429–1429, doi:10.1126/science.1108142, 2005.

Strack, M. and Waddington, J. M.: Response of peatland carbon dioxide and methane fluxes to a water table drawdown experiment, Global Biogeochem. Cy., 21, 13, GB1007, doi:10.1029/2006gb002715, 2007.

Tanaka, K., Tamagawa, I., Ishikawa, H., Ma, Y. M., and Hu, Z. Y.: Surface energy budget and closure of the eastern Tibetan Plateau during the GAME-Tibet IOP 1998, J. Hydrol., 283, 169–183, doi:10.1016/s0022-1694(03)00243-9, 2003.

Trenberth, K. E., Jones, P. D., Ambenje, P., Bojariu, R., Easterling, D., Klein Tank, A., Parker, D., Rahimzadeh, F., Renwick, J. A., Rusticucci, M., B., S., and Zhai, P.: Observations: Surface and Atmospheric Climate Change, in: Climate Change 2007: The Physical Science Basis. Climate Change 2007: The Physical Science Basis, edited by: Solomon, S., Qin, D., Manning, M., Chen, Z., Marquis, M., Averyt, K. B., Tignor, M., and Miller, H. L., Cambridge University Press, Cambridge, United Kingdom and New York, NY, USA, 2007.

von Fischer, J. C., Rhew, R. C., Ames, G. M., Fosdick, B. K., and von Fischer, P. E.: Vegetation height and other controls of spatial variability in methane emissions from the Arctic coastal tundra at Barrow, Alaska, J. Geophys. Res., 115, G00I03, doi:10.1029/2009jg001283, 2010.

Vourlitis, G. L., Oechel, W. C, Hastings, S. J., and Jenkins, M. A.: The effect of soil moisture and thaw depth on CH_4 flux from wet sedge tundra ecosystems on the North Slope of Alaska, Chemosphere, 26, 329-337, 1993.

Vourlitis, G. L., Oechel, W. C., Hastings, S. J., and Jenkins, M. A.: The effect of soil-moisture and thaw depth on CH_4 flux from wet coastal tundra ecosystems on the North Slope of Alaska (Vol. 26, 329, 1993), Chemosphere, 28, R1-R3, 1994.

Walker, D. A., Jia, G. J., Epstein, H. E., Raynolds, M. K., Chapin, F. S., Copass, C., Hinzman, L. D., Knudson, J. A., Maier, H. A., Michaelson, G. J., Nelson, F., Ping, C. L., Romanovsky, V. E., and Shiklomanov, N.: Vegetation-soil-thaw-depth relationships along a Low-Arctic bioclimate gradient, Alaska: Synthesis of information from the ATLAS studies, Permafrost and Periglacial Processes, 14, 103–123, doi:10.1002/ppp.452, 2003.

Walter, B. P. and Heimann, M.: A process-based, climate-sensitive model to derive methane emissions from natural wetlands: Application to five wetland sites, sensitivity to model parameters, and climate, Global Biogeochem. Cy., 14, 745–765, 2000.

Webb, E. K., Pearman, G. I., and Leuning, R.: Correction of flux measurements for density effects due to heat and water-vapor transfer, Q. J. Roy. Meteor. Soc., 106, 85–100, 1980.

Whalen, S. C. and Reeburgh, W. S.: Consumption of atmospheric methane by tundra soils, Nature, 346, 160–162, 1990.

Whalen, S. C. and Reeburgh, W. S.: Interannual variations in tundra methane emission: A 4-year time series at fixed sites, Global Biogeochem. Cy., 6, 139–159, doi:10.1029/92gb00430, 1992.

Wille, C., Kutzbach, L., Sachs, T., Wagner, D., and Pfeiffer, E. M.: Methane emission from Siberian arctic polygonal tundra: eddy covariance measurements and modeling, Global Change Biol., 14, 1395–1408, doi:10.1111/j.1365-2486.2008.01586.x, 2008.

Wilson, K., Goldstein, A., Falge, E., Aubinet, M., Baldocchi, D., Berbigier, P., Bernhofer, C., Ceulemans, R., Dolman, H., Field, C., Grelle, A., Ibrom, A., Law, B. E., Kowalski, A., Meyers, T., Moncrieff, J., Monson, R., Oechel, W., Tenhunen, J., Valentini, R., and Verma, S.: Energy balance closure at FLUXNET sites, Agr. Forest Meteorol., 113, 223–243, 2002.

Zona, D., Oechel, W. C., Kochendorfer, J., U, K. T. P., Salyuk, A. N., Olivas, P. C., Oberbauer, S. F., and Lipson, D. A.: Methane fluxes during the initiation of a large-scale water table manipulation experiment in the Alaskan Arctic tundra, Global Biogeochem. Cy., 23, GB2013, doi:10.1029/2009gb003487, 2009.

Table 1. Statistically significant environmental predictors of half-hourly autumn CH_4 flux. Results are from a forward-stepwise general linear model using the combined data from all three manipulation sections.

Variable	ΔR^2	F	p-value
Soil moisture (top 30 cm)	62.3 %	403.6	< 0.001
Wind speed x soil moisture	3.5 %	278.0	< 0.001
Soil temperature (20 cm depth)	2.6 %	98.8	< 0.001
Incoming shortwave radiation (310–2800 nm)	1.6 %	77.3	< 0.001
Total ($N = 1468$)	70.0 %		

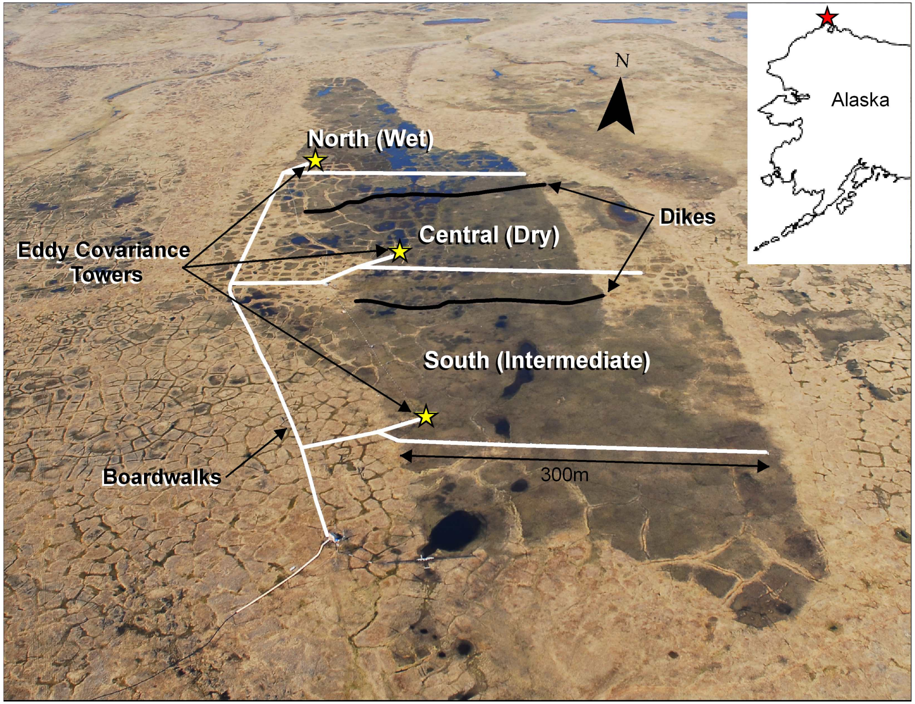

Fig. 1. Oblique aerial view of the Biocomplexity Experiment site. Note that scale changes throughout this image.

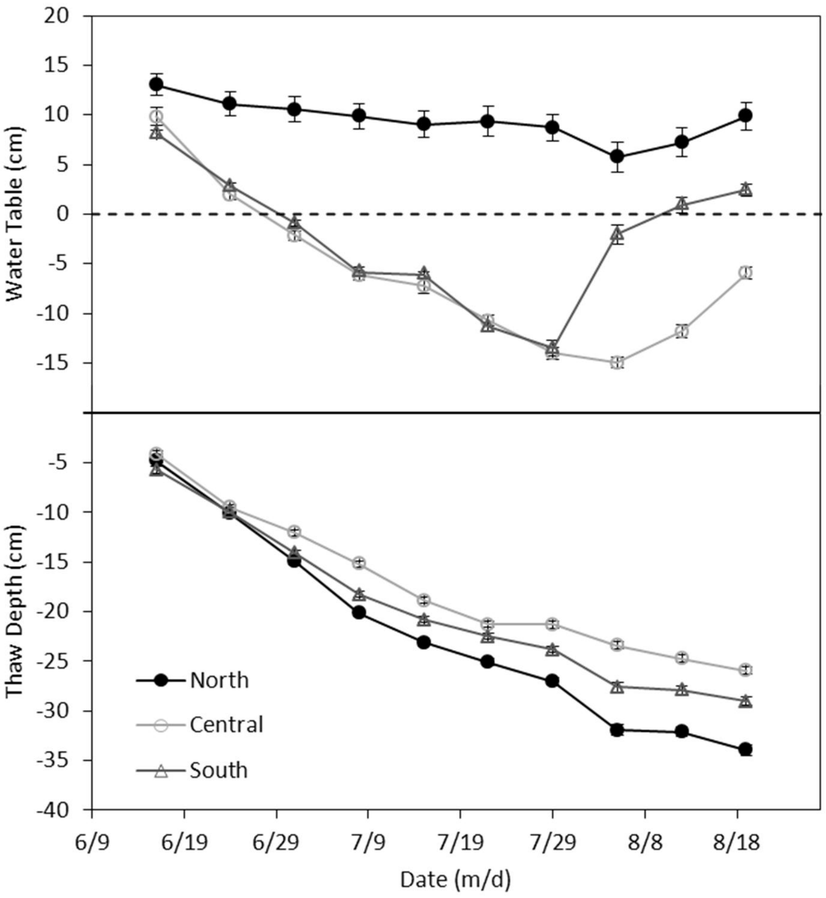

Fig. 2. Water table (top) and thaw depth (bottom) during the regular growing season of 2009. Points represent averages of measurements taken every 4 meters along the entire length of the boardwalks in each section. Negative values indicate positions below the surface. Error bars show standard error of the mean.

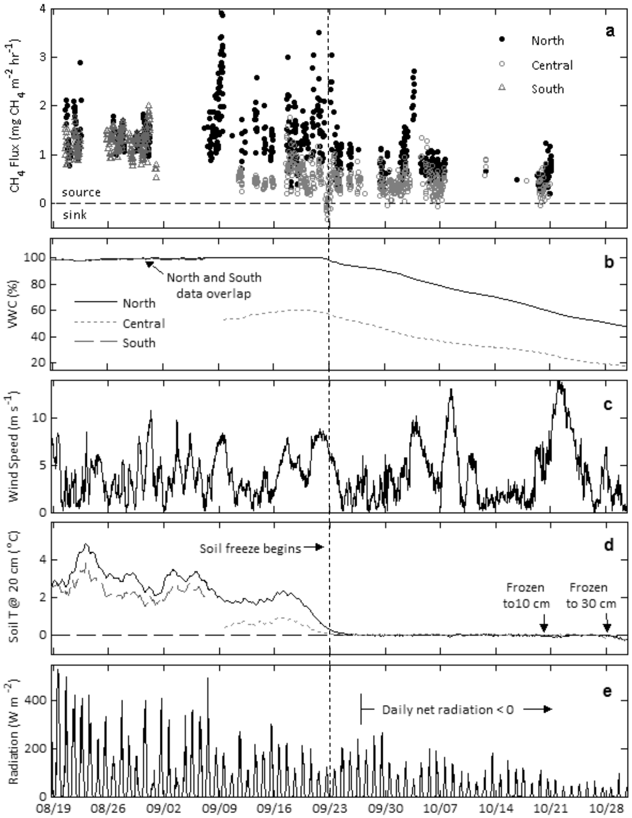

Fig. 3. Methane fluxes and selected environmental measurements recorded during the autumn. All displayed methane fluxes (panel a) passed quality control and originate within the respective manipulation footprints. Methane instruments were removed from the site on 25 October but axes are extended to show soil freeze to 30 cm depth on 28 October. With the exception of the extended plot period, the plotted periods of soil mosture in the top 30 cm (panel b) and soil temperature at 20 cm depth (panel d) for the Central and South sections are constrained to the duration of methane instrument installation. Wind speed (panel c) and incoming global shortwave radiation (310–2800 nm; panel e) are shown only for the Central section due to nearly equal values concurrently measured in the North and South sections.

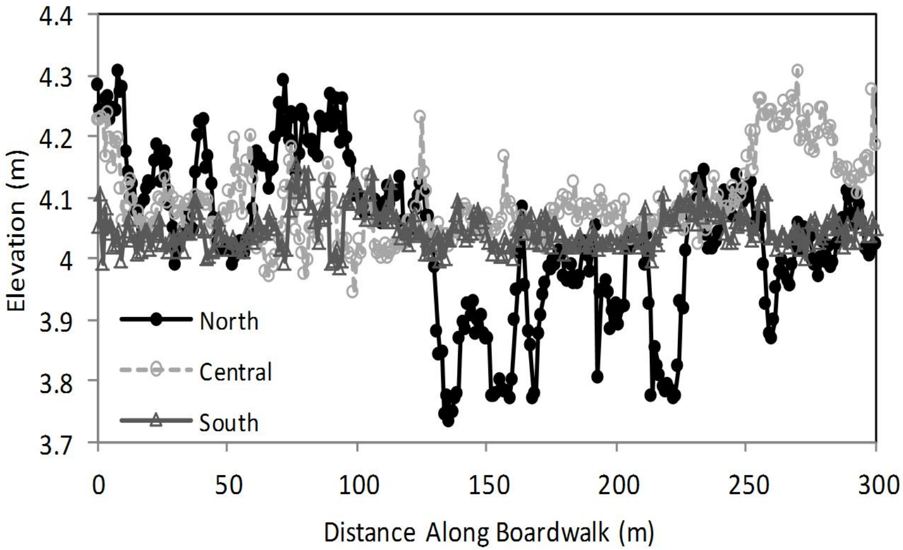

Fig. 4. Surface elevation (ASL) along the east-west boardwalk in each manipulation section. Note the greater microtopographic variation in the North section.